Binding Energies for Doubly-Charged Ions $M^{2+} = Mg^{2+}$, Ca^{2+} and Zn^{2+} with the Ligands L = H_2O, Acetone and *N*-methylacetamide in Complexes ML_n^{2+} for $n = 1$ to 7 from Gas Phase Equilibria Determinations and Theoretical Calculations

Michael Peschke, Arthur T. Blades, and Paul Kebarle*

Contribution from the Department of Chemistry, University of Alberta, Edmonton, Alberta, Canada T6G 2G2

Received June 6, 2000

Abstract: Experimental and theoretical binding energies, entropies, and free energies are reported for $M(L)_n^{2+}$ complexes, where M = Zn, Mg, Ca and L = acetone (Me_2CO) and *N*-methylacetamide (MAcA), as well as water for comparison. For the theoretical binding energies, expressed as dissociation energies ($\Delta H^\circ_{n,n-1}$), *n* extends up to 3 for the Mg-Me_2CO system, while for the experimental binding energies, *n* starts as low as 5 for the Zn- and Mg-acetone systems and reaches as high as 9 for the Ca(MAcA) system. For $n = 1$ complexes, Zn exhibits the strongest binding (due to sdσ hybridization and charge transfer), followed by Mg and then Ca (primarily electrostatic binding, with Mg being smaller). For the ligands, the trend based on dipole and polarizability holds for $n = 1$, with MAcA exhibiting the strongest binding, followed by Me_2CO and then H_2O. However, as *n* increases, the bond enthalpies drop at rates that cause them to equalize within a few kcal/mol for $n = 6$. The observed trend of bond enthalpy equalization has been attributed to primarily ligand−ligand repulsion in the case of Mg and Ca complexes. For the Zn complexes, loss of sdσ hybridization and charge-transfer play an added role so that, for example, for $Zn(H_2O)_3^{2+}$ and $Zn(H_2O)_4^{2+}$, the binding energies are lower than for the Mg analogues, despite the shorter bond distance in the Zn complexes. The experimental bond enthalpy and entropy differences for $M(Me_2CO)_n^{2+}$, where M = Ca and Mg and $n = 6$ and 7, show a sharp drop that corresponds to a transition to an outer shell for the seventh Me_2CO ligand. The entropies for the addition of the seventh ligand are much smaller than for the sixth ligand and correspond to a ligand that, due to the absence of ligand−ligand bonding interactions, is free to translate across the entire inner shell. The lower bond enthalpy and entropy for Zn as compared to Ca and Mg indicate that the transition to an outer shell is earlier for Zn. The strong hydrogen bonding between outer-shell and inner-shell MAcA ligands, indicated for $Ca(MAcA)_7^{2+}$, allows earlier transitions to an outer shell for Zn- and Mg-MAcA complexes as compared to their acetone analogues. Implications of the ligand interactions in the experimentally observed Ca complexes to Ca-containing proteins is also discussed.

I. Introduction

In a recent study,[1] we presented results from gas-phase ion−molecule equilibria measurements which led to the successive free energy changes: $\Delta G^\circ_{n-1,n}$, enthalpy $\Delta H^\circ_{n-1,n}$, and entropy $\Delta S^\circ_{n-1,n}$ for the hydration reactions of the doubly charged alkaline earth ions $M^{2+} = Mg^{2+}$, Ca^{2+}, Sr^{2+}, and Ba^{2+}.

$$M(H_2O)_{n-1}^{2+} + H_2O = M(H_2O)_n^{2+} \qquad (1)$$

In the present work, the equilibrium measurements were extended to include the biochemically important Mg^{2+}, Ca^{2+}, and Zn^{2+} and the ligands L = acetone (Me_2CO) and *N*-methylacetamide MeCONHMe (MAcA).

$$M(Me_2CO)_{n-1}^{2+} + Me_2CO = M(Me_2CO)_n^{2+} \qquad (2)$$

$$M(MAcA)_{n-1}^{2+} + MAcA = M(MAcA)_n^{2+} \qquad (3)$$

MAcA was chosen because it is the simplest model for peptide backbone interactions.[2,3] Comparisons of the bonding of MAcA with acetone provide useful insights into the effect of the NHMe group on the carbonyl oxygen−metal ion interactions. The earlier results obtained for the $M^{2+}-(H_2O)_n$ interactions[1] are also useful in the present context because they are a measure of the stability provided by the hydration interactions relative to that of the interactions with ligands such as MAcA. This comparison is of special importance because in metalloenzymes, the bonding of the metal ion to ligands of the protein must be strong relative to that with water to provide stability of the metal ion in the enzyme relative to that in aqueous solution.

As was the case in the previous work on the hydration of the doubly charged ions,[1] only equilibrium determinations for $n > 5$ were possible because the bond energies for the lower *n* are very high and require very high temperatures for the determi-

(1) Peschke, M.; Blades, A. T.; Kebarle, P. *J. Phys. Chem. A* **1998**, *102*, 9978.

(2) (a) Roux, B.; Karplus, M. *Biophys. J.* **1991**, *59*, 961. (b) Roux, B.; Karplus, M. *J. Phys. Chem.* **1991**, *95*, 4856. (c) Roux, B.; Karplus, M. *J. Am. Chem. Soc.* **1993**, *115*, 3250.

(3) Klassen, J. S.; Anderson, S. G.; Blades, A. T.; Kebarle, P. *J. Phys. Chem.* **1996**, *100*, 14218.

10.1021/ja002021z CCC: $19.00
Published on Web 10/05/2000

nation of the equilibria. Such temperatures are not accessible with the apparatus that was used.[1,4] Fortunately, theoretical calculations providing quite reliable successive energy and entropy change values, $\Delta G^\circ_{n-1,n}$, $\Delta H^\circ_{n-1,n}$ and $\Delta S^\circ_{n-1,n}$ at low n, are now possible. For the hydration reactions, a set of results by Siegbahn and co-workers,[5] obtained by density functional theory (DFT), were available up to $(n-1, n) = (6, 7)$, and the equilibrium results provided data from (5, 6) to (13, 14). Generally good agreement was found[1] in the range (5, 6)−(6, 7) where the experimental and theoretical data overlapped. A combination of the two sets of results was found to provide a comprehensive description of the hydration interactions.[1]

For the ligands L = Me_2CO and MAcA and Mg^{2+}, Ca^{2+}, and Zn^{2+}, only sparse theoretical data are available in the literature. Therefore, calculations at the B3LYP/6-311++G-(d,p) level were performed in this laboratory. Due to the much greater complexity of Me_2CO and MAcA in comparison to the water molecule, the range of successive energies $(n-1, n)$ accessible to computation was much smaller. The calculations could be extended up to $(n-1, n) = (2, 3)$ only for the computationally simpler system Mg^{2+} and Me_2CO. For the other systems, only the (0, 1) and occasionally the (1, 2) values could be obtained. Nevertheless, a combination of the theoretical results for low n and the experimental results for high n provides, as will be seen, some valuable insights into the bonding of these ligands.

IIa. Experimental Section

The equilibrium determinations were performed using the ion-reaction chamber that was previously described.[4] Briefly, the ions were produced by the electrospray[6] of solutions of the MCl_2 salts in methanol at concentrations of $10^{-4}-10^{-3}$ mol/L at flow rates of less than 0.5 μL/min. The ions produced by electrospray in the atmospheric air were transferred into nitrogen gas and introduced through a capillary into a forechamber where the nitrogen pressure was 10 Torr. An imposed weak electric field caused the ions to drift into a reaction chamber which contained nitrogen gas at 10 Torr and known partial pressures of ligand L vapor P_L, in the 1−100 mTorr range. The reaction chamber was sampled by letting gas and ions escape through an orifice that led to an evacuated chamber and a triple quadrupole mass spectrometer. The intensity ratio I_n/I_{n-1} for the ions ML_n^{2+} and ML_{n-1}^{2+}, was determined at several partial pressures P_L of the ligand vapor and plots of I_n/I_{n-1} versus P_L led to straight lines as required by the equilibrium expression:

$$K_{eq} = \frac{I_n \cdot 760\ \text{Torr}}{I_{n-1} P_L} \qquad (4)$$

where the ion intensity ratio is assumed to be proportional to the ion partial pressure ratio in the reaction chamber.[4] The equilibrium constants $K_{eq} = K_{n-1,n}$ obtained from the slope of these plots (see eq 4), were used for the van't Hoff plots given in Figures 1−3. The slopes of the straight lines that were obtained correspond to the enthalpy change $\Delta H^\circ_{n-1,n}$, and the intercepts lead to the entropy change $\Delta S^\circ_{n-1,n}$. These values, together with the free energy change, $\Delta G^\circ_{n-1,n} = \Delta H^\circ_{n-1,n} - T\Delta S^\circ_{n-1,n}$, are given in Table 1. To avoid the minus sign for energy and entropy changes that occur for addition reactions, the values are given as dissociation energies and entropies ($\Delta G^\circ_{n,n-1}$, $\Delta H^\circ_{n,n-1}$, and $\Delta S^\circ_{n,n-1}$).

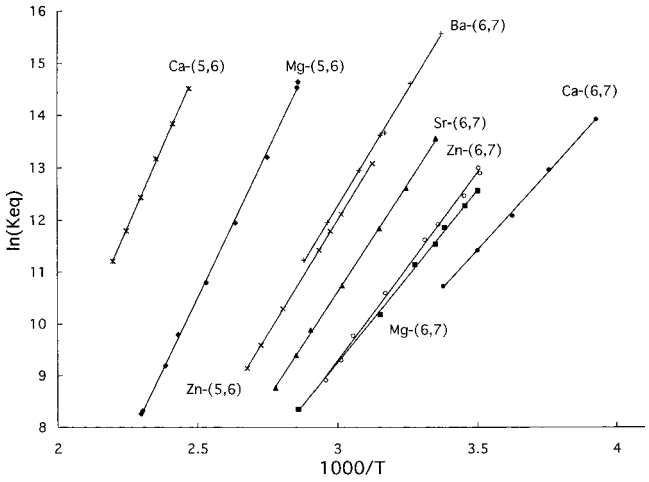

Figure 1. van't Hoff plots involving equilibrium constants, $K_{eq} = K_{n-1,n}$ of equilibria: $ML_{n-1}^{2+} + L = ML_n^{2+}$ for M = Mg^{2+}, Ca^{2+}, Zn^{2+}, Sr^{2+}, and Ba^{2+} and L = acetone. Because the equilibrium determinations were performed over roughly the same range of ligand partial pressures, plots shifted to the right (low temperature) correspond to weak ion-ligand bond free energy. Notable is the reversal $(n-1, n)$ in the order of Ca (5,6), Mg (5,6), and Zn (5,6) relative to the order of Zn, which is stronger bonding than Mg, which is stronger bonding than Ca, that is observed at $n = 1$, see Table 1.

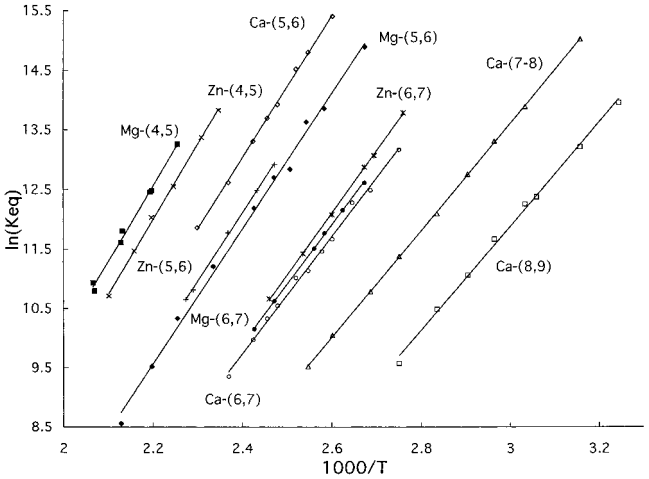

Figure 2. van't Hoff plots involving equilibrium constants $K_{eq} = K_{n-1,n}$ of equilibria $ML_{n-1}^{2+} + L = ML_n^{2+}$ for Mg^{2+}, Ca^{2+}, and Zn^{2+} and L = *N*-methyl acetamide (MAcA). Note very different results for MAcA when compared to acetone results in Figure 1.

IIb. Computational Methods

All computations in this study were done using the Gaussian94[7] suite of programs. Due to the large number of atoms involved in some of the ion-ligand complexes and the necessity of a common computational level to facilitate comparisons, the B3LYP set of DFT functionals was chosen. This model has been shown in many studies to be generally of a reliability comparable to the MP2 method,[8] while requiring far less disk space and being fast enough to allow the computations undertaken in this study. In addition, previous studies have shown that the B3LYP model is very well-suited for ion−ligand complexes, the systems of interest.[5,8b,9]

(4) Blades, A. T.; Klassen, J. S.; Kebarle, P. *J. Am. Chem. Soc.* **1996**, *118*, 12437.

(5) Pavlov, M.; Siegbahn, P. E.; Sandström, M. *J. Phys. Chem. A* **1998**, *102*, 219.

(6) (a) Fenn, J. B.; Mann, M.; Meng, C. K.; Wong, S. F.; Whitehouse, C. M. *Science* **1985**, *246*, 64. (b) Kebarle, P.; Tang, L. *Anal. Chem.* **1993**, *65*, 972A.

(7) Frisch, M. J.; Trucks, G. W.; Schlegel, H. B.; Gill, P. M.; Johnson, P. M.; Robb, M. A.; Cheeseman, J. R.; Keith, T.; Petersson, G. A.; Montgomery, J. A.; Raghavachari, K.; Al-Laham, M. A.; Zakrzewski, V. G.; Ortiz, J. V.; Foresman, J. B.; Cioslowski, J.; Stefanov, B. B.; Nanayakkara, A.; Challacombe, M.; Peng, C. Y.; Ayala, P. Y.; Chen, W.; Wong, M. W.; Andres, J. L.; Replogle, E. S.; Gomperts, R.; Martin, R. L.; Fox, D. J.; Binkley, J. S.; Defrees, D. J.; Baker, J.; Stewart, J. P.; Head-Gordon, M.; Gonzalez, C.; Pople, J. A. *Gaussian 94*, Revision D.3; Gaussian, Inc.: Pittsburgh, PA, 1995.

Table 1. Bonding Energies[a] of Acetone (Me_2CO) and *N*-Methylacetamide (MAcA) to Mg^{2+}, Ca^{2+} and Zn^{2+} for the Reaction $M(L)_{n-1}^{2+} + L \rightarrow M(L)_n^{2+}$

	Zn			Mg			Ca		
	$\Delta H°_{298}$[c]	$\Delta S°_{298}$	$\Delta G°_{298}$	$\Delta H°_{298}$[c]	$\Delta S°_{298}$	$\Delta G°_{298}$	$\Delta H°_{298}$[c]	$\Delta S°_{298}$	$\Delta G°_{298}$
				L = H_2O[b]					
1,0 (th)	103.1 (101.9)	22.6	96.3	81.8 (81.5)	24.2	74.6	56.5 (56.9)	23.4	49.5
2,1 (th)	88.0 (86.6)	33.4	78.1	72.0 (70.9)	28.9	63.4	48.5 (47.5)	20.8	42.3
3,2 (th)	55.8 (53.6)	25.2	48.3	56.6 (55.1)	26.6	48.7	42.9 (42.0)	28.5	34.4
4,3 (th)	42.9 (41.2)	28.9	34.3	(43.9)			(35.6)		
5,4 (th)	(25.0)			(28.0)			(27.7)		
6,5 (th)	(24.2)			(24.0)			(24.7)		
6,5 (ex)				24.6	29.1	16.0	25.3	31.1	16.1
7,6 (th)				(19.0)			(17.6)		
7,6 (ex)				20.3	25.3	12.8	16.9	20.2	10.9
				L = Me_2CO					
1,0 (th)	153.5	27.5	145.3	121.2	27.3	113.0	89.3	27.6	81.1
2,1 (th)	104.9	34.3	94.7	95.0	28.9	86.4			
3,2 (th)				63.3	39.3	51.5			
6,5 (ex)	17.4	28.5	9.0	22.3	34.8	11.9	24.2	30.9	15.0
7,6 (ex)	14.4	24.6	7.0	13.6	22.4	6.9	11.6	17.8	6.3
				L = MacA					
1,0 (th)	174.9	31.0	165.7	140.9	28.9	132.3	106.5	29.3	97.7
2,1 (th)				107.8	36.6	96.9			
5,4 (ex)	25.1	31.4	15.8	25.3	30.6	16.1			
6,5 (ex)	22.9	30.8	13.7	22.6	30.8	13.5	23.7	30.9	14.5
7,6 (ex)	20.8	29.9	11.8	19.9	28.1	11.5	19.6	27.7	11.3
8,7 (ex)							17.9	26.5	10.0
9,8 (ex)							17.5	29.0	8.9

[a] All energies are given in kcal/mol, and the entropies are given in cal/mol·K. The standard level for all computational values is B3LYP/6-311++G(d,p) unless otherwise noted. [b] Theoretical values are denoted by (th) and experimental values by (ex). [c] Values in parentheses are bond energies at 0 K from Pavlov, M.; Siegbahn, P. E. M.; Sandström, M. *J. Phys. Chem. A* **1998**, *102*, 219

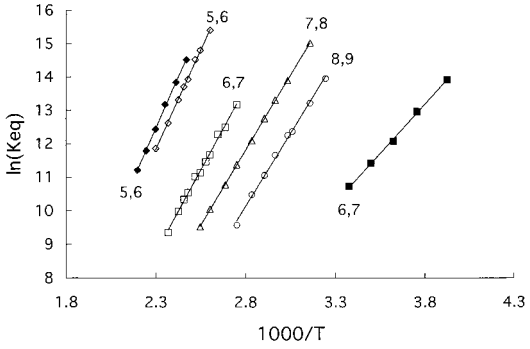

Figure 3. van't Hoff plots for Ca^{2+}, acetone (blackened symbols), and Ca^{2+} *N*-methylacetamide MAcA (open symbols). Plots shifted to the right (low temperature) indicate weaker bonding. Note relatively much stronger bonding with MAcA for (6,7), (7,8), and (8,9), while (6,7) bonding with acetone is much weaker than all of the above. Observed difference for acetone and MAcA is due to hydrogen bonding between inner (six shell) and outer $n > 6$ MAcA molecules, which is absent for acetone.

Previous studies in our lab[9a] with the 6-311++G(d,p) basis set have led to energy values in good agreement with experimental results. This basis set contains sufficient diffuse functions and is flexible enough to give a good account of the longer ranging ion−ligand interactions. In addition, this basis set is large enough to generally reduce the basis set superposition error for the relatively large ion−ligand bond energies (>20 kcal/mol) below the error bars inherent in the method and, thus, making superposition error corrections unnecessary. On the other hand, such a basis set leads to time-consuming calculations for the larger ion−molecule complexes, making it desirable to use a smaller basis set for the optimization part and then to use single-point energy calculations with the larger basis set. Such an approach was used successfully by Pavlov et al.[5] in their study of $M(H_2O)_n^{2+}$ complexes. The basis set used by Pavlov et al. for the optimization portion was the LANL2DZ set, an effective core-potential basis set. To see if such an approach could be used also for our study, $Mg(Me_2CO)_n^{2+}$ and $Zn(Me_2CO)_n^{2+}$ were used as test systems. While the energies for the $Mg(Me_2CO)_n^{2+}$ systems at the B3LYP/6-311++G(d,p)//LANL2DZ level differed by no more than 0.6 kcal/mol from those optimized at the B3LYP/6-311++G(d,p) level, for the $Zn(Me_2CO)_n^{2+}$ complexes, the optimizations with the LANL2DZ basis set led to much larger energy and geometry differences. Because the 6-311++G(d,p) basis set is larger and more flexible than the LanL2DZ set, it is more likely to provide a correct description of the interactions. Our conclusion regarding the use of the LanL2DZ basis set for metal ion-ligand systems is that it is adequate for complexes with primarily electrostatic interactions, which is expected with Ca^{2+} and Mg^{2+}, but is not adequate for complexes, as with Zn^{2+}, that exhibit more complicated orbital and charge-transfer interactions. Therefore, the B3LYP/6-311++G(d,p) level was used as the standard level for optimizations as well as frequency calculations for all complexes except for the largest $Ca(MAcA)_n^{2+}$ complexes where the LanL2DZ set was used for optimization. In addition, for the high level calculations of Ca, the only element in this study not included in the 6-311++G(d,p) basis set, the valence triple-ζ basis set by Ahlrichs[10] supplemented with two contracted *d* polarization functions [0.43·*d*(1.97) + 1.0·*d*(0.40)][11] was used. Inclusion

(8) (a) Wiberg, K. B.; Ochterski, J. W. *J. Comput. Chem.* **1997**, *18*, 108. (b) Ṣmith, B. J.; Radom, L. *Chem. Phys. Lett.* **1994**, *231*, 345. (c) Hobza, P.; Ṣponer, J.; Reschel, T. *J. Comput. Chem.* **1995**, *16*, 1315. (d) González, L.; Mó, O.; Yáñez, M. *J. Comput. Chem.* **1997**, *18*, 1125. (e) Kafafi, S. A.; Krauss, M. *Int. J. Quantum Chem.* **1999**, *75*, 289.

(9) (a) Peschke, M.; Blades, A. T.; Kebarle, P. *J. Am. Chem. Soc.* **2000**, *122*, 1492. (b) Stöckigt, D. *Chem. Phys. Lett.* **1996**, *250*, 387.

(10) (a) Schafer, A.; Horn, H.; Ahlrichs, R. *J. Chem. Phys.* **1992**, *97*, 2571. (b) Basis sets were obtained from the Extensible Computational Chemistry Environment Basis Set Database, Version 1.0, as developed and distributed by the Molecular Science Computing Facility, Environmental and Molecular Sciences Laboratory, which is part of the Pacific Northwest Laboratory, P. O. Box 999, Richland, WA 99352, and funded by the U.S. Department of Energy. The Pacific Northwest Laboratory is a multi-program laboratory operated by Battelle Memorial Institue for the U.S. Department of Energy under contract DE-AC06−76RLO 1830. Contact David Feller, Karen Schuchardt, or Don Jones for further information.

(11) (a) Peschke, M.; Blades, A. T.; Kebarle, P. *Int. J. Mass Spec. Ion Proc.* **1999**, *185/186/187*, 685. (b) Garmer, D. R.; Gresh, N. *J. Am. Chem. Soc.* **1994**, *116*, 3556.

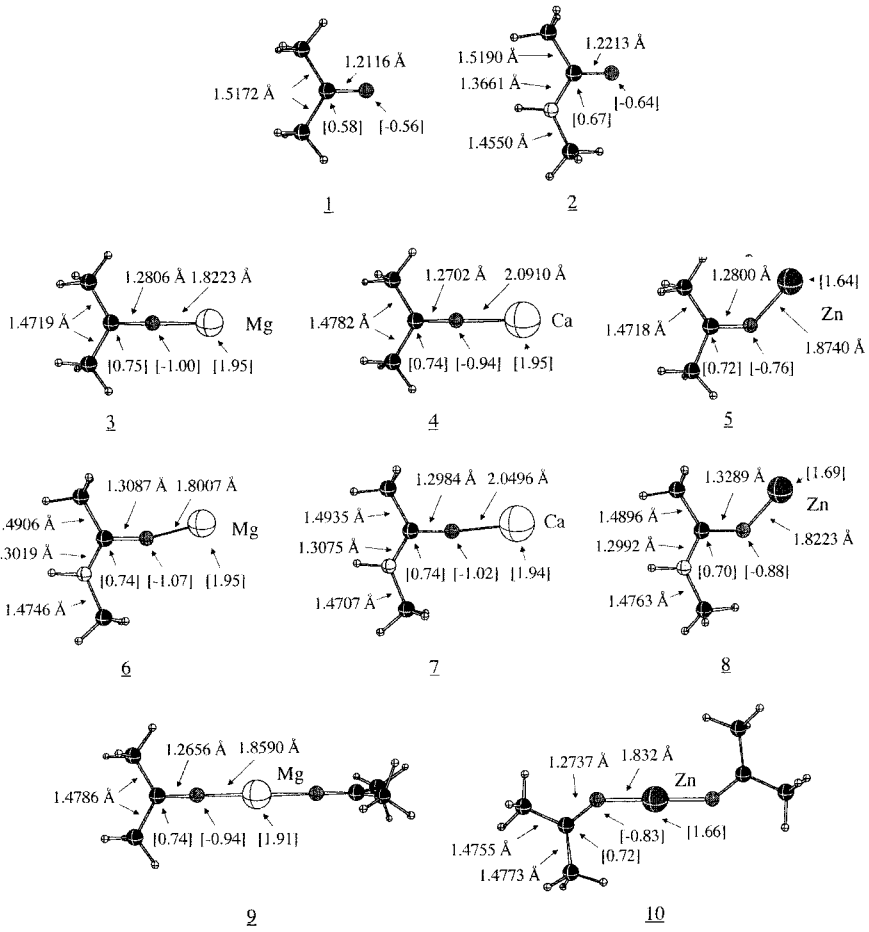

Figure 4. Theoretical geometries of various ligand and ion-ligand complexes at the B3LYP/6-311++G(d,p) level. Values in brackets are atomic charges from NPA. 1, Acetone (Me_2CO); 2, *N*-methylacetamide (MAcA); 3, $Mg(Me_2CO)^{2+}$; 4, $Ca(Me_2CO)^{2+}$; 5, $Zn(Me_2CO)^{2+}$; 6, $Mg(MAcA)^{2+}$; 7, $Ca(MAcA)^{2+}$; 8, $Zn(MAcA)^{2+}$; 9, $Mg(Me_2CO)_2^{2+}$; 10, $Zn(Me_2CO)_2^{2+}$

of the polarization functions is essential, because computational results without the polarization functions can differ by more than 30 kcal/mol.

As pointed out in a previous paper,[9a] ions with two or more moderately large ligands tend to lead to difficulties in meeting the displacement optimization criteria. This was attributed to the overall potential energy surface (PES) of the complexes being flat around the energy minimum yet still exhibiting many small energy barriers (<0.1 kcal/mol), which is probably due to a number of competing long-range interactions. From a practical standpoint, the obtained energy values from the flat PES portion are entirely adequate because the energy deviations are less than 0.1 kcal/mol and the entire PES portion is expected to be sampled at experimental temperatures. However, entropy determinations, which rely on the frequencies, are also of interest in the present work. Due to the incomplete optimization in some of the calculations, one or more of the frequencies obtained for those complexes can be negative and would correspond to cases in which the complex has one or more degrees of freedom close to some of the many small energy bumps on the PES. Had a complete geometry optimization been achieved, these frequencies would be expected to be very small. The zero-point energy determination would, therefore, not be affected, because the very small frequencies make a negligible contribution. However, entropy and heat capacity evaluations would be affected and could, therefore, not be performed for those systems. But this is not a big disadvantage, because obtaining reliable entropies for complexes which contain a number of hindered rotors as those present here is not easy in any case. To compute entropy contributions for hindered rotors, one cannot use those frequencies directly but must use a separate hindered rotors procedure.[12] For large complexes, it is not easy to separate hindered rotor contributions from other mixed-in vibrational modes. Moreover, because the PES is flat enough that the complex can sample a larger portion of the PES than just one particular local minimum, an entropy evaluation would have to account for that, as well, and would require an even more involved procedure.

To gain additional understanding, especially with regard to possible charge-transfer interactions of the ligand to the metal cation center, natural population analysis[13] (NPA) was carried out, as well. NPA decomposes the orbital space from the arbitrary atomic input set into an orthonormal "natural atomic orbital" (NAO) set. This set, due to its occupancy weighting criteria, consists of high-occupancy one-center orbitals that correspond to a minimal set that describes the atomic subshells of the electronic ground state of the particular center plus low-occupancy Rydberg orbitals. The interatomic overlap has been removed via the NAO symmetry orthogonalization procedure. Adding up the occupancies of the orbitals around one atom yields the charge of that atom. These atomic charges are very consistent once a sufficiently large basis set has been reached. It is well-known that charges based on Mulliken population analysis tend to be unreliable with respect to basis set expansion.[13] In addition, due to the even division of the orbital overlap population in Mulliken, bond polarization is not taken into account. This can lead to a distorted picture of the calculated atomic charges. Consequently, NPA was used for all charge determinations in the text.

III. Results and Discussion

(a) Structures and Energy of Ion−Ligand Complexes Obtained from Theoretical Calculations. The structures for the most germane complexes are shown in Figure 4,[14] which

(12) See for example: East, A. L. L.; Smith, B. J.; Radom, L. *J. Am. Chem. Soc.* **1997**, *119*, 9014.

(13) Reed, A. E.; Weinstock, R. B.; Weinhold, F. *J. Chem. Phys.* **1985**, *83*, 735.

Table 2. Atomic Charges (NPA) on the Metal Center and Adjoining Oxygen and Distance between Them

	$Zn(L)_n^{2+}$			$Mg(L)_n^{2+}$			$Ca(L)_n^{2+}$		
	q(Zn)	q(O)	Zn−O(Å)	q(Mg)	q(O)	Mg−O(Å)	q(Ca)	q(O)	Ca−O(Å)
					L = H_2O				
1	1.89	−1.08	1.8832	1.96	−1.12	1.9428	1.97	−1.09	2.2500
2	1.76	−1.05	1.8771	1.91	−1.09	1.9590	1.96	−1.07	2.285
3	1.76	−1.05	1.9463	1.87	−1.07	1.9875	1.93	−1.06	2.3172
4	1.76	−1.03	2.003						
					L = Me_2CO				
1	1.65	−0.76	1.8740	1.95	−1.00	1.8223	1.95	−0.94	2.0910
	(1.86)[a]	(−0.99)	(1.7730)						
2	1.66	−0.83	1.8320	1.91	−0.94	1.8590			
3				1.88	−0.87	1.9090			
					L = MacA				
1	1.69	−0.88	1.8223	1.95	−1.07	1.8007	1.94	−1.02	2.0496
2				1.91	−1.01	1.8401			

[a] Values in parentheses refer to the linear $Zn(Me_2CO)^{2+}$ complex.

includes also the structures of Me_2CO and MAcA that are given for comparison. The binding enthalpies, entropies, and free energies are given in Table 1 and also include energy values for water as a ligand for comparison. Calculated atomic charges on the metal cation and the adjoining oxygen, as well as the metal−oxygen bond distance, are given in Table 2.

Two general trends can be observed for the $n = 1$ complexes. The bond enthalpies increase in the order of Ca, Mg, and Zn for all three ligands, and the bond enthalpies increase in the order of H_2O, Me_2CO, and MAcA for all three metal cations. However, as n increases, these differences disappear and the trends can actually reverse (see $\Delta H^\circ_{6,5}$ for Me_2CO in Table 1). The computational part of this study probes the cause for these trends and their change.

Primary Ligand Differences. The theoretically predicted trend of increasing bond enthalpies in the order of H_2O, Me_2CO, and MAcA, see Table 1, is expected. The same order has been experimentally observed,[3,15,16] and additionally for Cu^+, Na^+, and K^+, which are isoelectronic to Zn^{2+}, Mg^{2+}, and Ca^{2+}. Stronger electrostatic bonding of acetone would be expected from the larger dipole ($\mu_{acetone} = 2.88$ D, $\mu_{water} = 1.85$ D) and the increased polarizability ($\alpha_{acetone} = 6.33$ Å^3, $\alpha_{water} = 1.48$ Å^3). The effect of the polarization can be seen in the increased bond distance of the C−O bond in the $M(Me_2CO)^{2+}$ complexes as compared to the neutral Me_2CO (see structures 1 and 3−5), which corresponds to a loosening of the π bond and an increased negative charge on the oxygen.

Stronger bonding due to charge transfer can be expected also, because Me_2CO and MAcA have a lone pair orbital on the oxygen, which is a much better electron donor than is water. An approximate measure of the donor difference between water and acetone is provided by the ionization energies, which are 12.6 and 9.7 eV, respectively.[17]

The further increase in bond enthalpy from the Me_2CO complexes to the MAcA complexes is the result of electron donation from the nitrogen atom into the carbon p and C−O π bond orbital space. This leads to a higher computed polarizability and dipole moment for MAcA. The bond distance changes of the $M(MAcA)^{2+}$ complexes (structures 6−8) as compared to neutral MAcA (structure 2) are strong evidence of the electron shift. The N−C bond has been decreased from 1.37 Å to between 1.30 and 1.31 Å, which is much closer to the C═N double bond distance of 1.26 to 1.27 Å in $RN{=}CR_2$ systems. At the same time, the C−O bond distance has increased to between 1.30 and 1.33 Å, which is much longer than the bond distance for the neutral MAcA (1.22 Å) and also longer than that of the C−O bond of the $M(Me_2CO)^{2+}$ complexes (1.27 to 1.28 Å).

Bond Enthalpy Trend Analysis. The contributions to the bond enthalpy of $M(L)_n^{z+}$ complexes can be roughly divided into (a) attractive electrostatic contributions, which include ion−dipole and ion−induced-dipole interactions and are expected to be the major contribution to the bond strength; (b) charge transfer from ligand to ion, which can be expected to be more significant for doubly, as compared to singly, charged ions and for more polarizable, strongly electron donating ligands; (c) electronic orbital effects such as ion core polarization and sdσ hybridization, as proposed by Bauschlicher for Cu^+;[18] (d) ion−ligand repulsion; and (e) ligand−ligand repulsion due to dipole−dipole and Pauli repulsion. This last contribution can be expected to become more important as n increases and will lead eventually to a transition to an outer shell.

The atomic charges (see Table 2) for the Ca and Mg complexes indicate that the amount of charge transfer is very small with no significant difference for any of the ligands, despite the more available electrons for charge transfer in Me_2CO and MAcA as compared to water. Apparently, the energy difference between the ligand HOMO and the LUMO on the Ca and Mg cation is still too large, so that the energy gain from charge transfer is too small to offset the resulting loss in electrostatic bonding. Mg and Ca are aligned with the dipole of Me_2CO (see structures 3 and 4), thus optimizing the electrostatic interaction. The same alignment can be observed for MAcA. In the $Mg(MAcA)^{2+}$ complex, the Mg−O−C angle is 165° (see structure 6), not 180°. The smaller angle is a consequence of the charge distribution in MAcA which leads to a dipole which is not exactly aligned with the C−O axis. A similar effect is present also for $Ca(MAcA)^{2+}$ (see structure 7). The predominant ion-ligand interaction for the Ca and Mg adducts, consequently, can be expected to be electrostatic. It will be, therefore, instructive to first compare the ion complexes of these two metals to understand why the initially large bond enthalpy differences converge. For the $n = 1$ complexes, the bond enthalpy increase from Ca to Mg is then expected simply on the basis of the smaller size of the Mg^{2+} ion and the subsequently stronger electrostatic contribution (see bond distances in Table 2). A simple ion−dipole, ion−induced-dipole

(14) Coordinates for all computed structures are available upon request.
(15) Deng, H.; Kebarle, P. *J. Am. Chem. Soc.* **1998**, *120*, 2925.
(16) Sunner, J.; Kebarle, P. *J. Am. Chem. Soc.* **1984**, *106*, 6135.
(17) Hunter, E. P.; Lias, S. G. *J. Chem. Phys. Ref. Data* **1998**, *27*, 3.
(18) Bauschlicher, C. W.; Langhoff, S. R.; Partridge, H. *J. Chem. Phys.* **1991**, *94*, 2068.

model indicates that the bond distance differences are entirely sufficient to explain the bond enthalpy differences for water and Me_2CO (for MAcA, the experimental polarizability constant, α, was not available).

For the $Ca(H_2O)_n^{2+}$ system, the biggest bond enthalpy drop is from $n = 1$ to $n = 2$, approximately 8−9 kcal/mol. Using a point charge model, Bauschlicher and co-workers estimated the water ligand repulsion for $Cu(H_2O)_2^{2+}$ at 1.6 kcal/mol.[18] For calcium, which has a larger bond distance to water (2.29 Å vs 2.04 Å[18]), the ligand−ligand repulsion would be less and, therefore, not the major contributor to the bond enthalpy drop. The most likely cause for the enthalpy lowering in this case is the reduction of the polarization of the electron distribution around the ion, now that there are two ligands, although Ca is able to maintain some of the polarization by keeping both ligands on one side with an angle of 118° between them, as has been shown previously.[11a,19] For more than two water ligands, however, Bauschlicher and co-workers showed that ligand−ligand repulsion becomes significant such as in the case of $Cu(H_2O)_3^{2+}$, where they have estimated the water−water repulsion to be about 11 kcal/mol.[18] For $Ca(H_2O)_3^{2+}$ the increased ligand−ligand repulsion results in an almost planar structure with all three ligands still on one side, indicating that the ligand−ligand repulsion is probably less than that for Cu^+ and is still competing with ion−core polarization effects. For $Mg(H_2O)_2^{2+}$, the bond enthalpy drop is of similar magnitude as that for $Ca(H_2O)_2^{2+}$, and the primary cause is also likely to be the loss of ion core polarization. The slight increase in the drop for Mg is consistent with a slightly higher dipole−dipole repulsion of the two water ligands, which causes them to be 180° apart and results in a less effective ion core polarization. The enthalpy drop from two water ligands to three water ligands is significantly larger for Mg than for Ca (15.4 vs 5.5; see Table 1).

Point charge calculations analogous to those done by Bauschlicher for $Cu(L)_n^+$ systems were performed for several select systems to estimate the magnitude of the ligand−ligand repulsion. However, the absolute values from point charge calculations are exaggerated, due to the absence of ion−ligand repulsion, which allows an unrealistically high ligand polarization, especially for doubly charged points. Nevertheless, the results from such point-charge calculations can be viewed as a maximum value for ligand−ligand repulsion and, as such, serve as a qualitative indicator. Due to the closer distances of the water ligands in $Mg(H_2O)_3^{2+}$ as compared to Ca (see Table 2), the ligand−ligand repulsion increases significantly. From the point-charge calculations, the ligand−ligand repulsion for the three waters in the Mg system is 28 kcal/mol, but it is only 11 kcal/mol for the Ca system. Even though the actual ligand−ligand repulsion is lower, the difference between the Mg and Ca complexes is probably sufficient to account for the large bond enthalpy drop for $Mg(H_2O)_3^{2+}$ as compared to Ca.

The bond enthalpy drop for the second ligand addition of Me_2CO and MAcA to Mg is larger than that for the analogous water case, as would be expected. The loss of ion polarization is energetically more significant for ligands with a larger dipole and higher polarizability. In addition, point-charge calculations indicate a maximum value of the ligand−ligand repulsion for $Mg(Me_2CO)_2^{2+}$ of 29 kcal/mol. While the actual ligand−ligand repulsion is lower, the numbers indicate a large increase for ligands such as Me_2CO and MAcA as compared to water and, together with the loss of ion polarization, could be sufficient to explain the enthalpy drops for addition of the second ligand. For the electrostatic complexes of Ca and Mg, the converging bond enthalpies as n increases can then be rationalized by the differences in ligand−ligand repulsion, which are more significant for Mg, for which the ligands are closer to each other.

Zn^{2+} allows more complex interactions than either Mg^{2+} or Ca^{2+}. Transition metals such as Cu^+, which is isoelectronic to Zn^{2+}, can undergo sdσ hybridization, as Bauschlicher and co-workers have pointed out,[18] and, as has been previously shown,[20] Zn^{2+} can do so, as well. This hybridization involves the 4s and $3d_{z^2}$ orbitals and, concomitant to the extent of the hybridization, the shape of the ds orbital that is occupied results in a transfer of electron density away from the lobes of the unhybridized $3d_{z^2}$ orbital. The decreased charge density lowers the ion−ligand repulsion along the z axis and allows ligands from that direction to approach closer, which increases favorable electrostatic contributions as well as orbital overlap between ligand orbitals and the empty sd hybridized orbital, thus facilitating possible charge transfer.

Zn^{2+} and Mg^{2+} are of similar size, so that a comparison of their complexes can illustrate the differences of primarily electrostatic binding and binding that involves a significant charge transfer in addition to the electrostatic contribution and how that difference might affect the rate of convergence of the bond enthalpies with increasing n.

In the case of $Zn(H_2O)^{2+}$, the sdσ orbital can accept an energetically favorable charge transfer from the water ligand, so that the combination of hybridization and charge transfer can rationalize the large bond enthalpy increase of 21.3 kcal/mol as compared to $Mg(H_2O)^{2+}$. The occurrence of charge transfer is supported by the atomic charge distribution on the Zn cation and adjoining oxygen (see Table 2). The atomic charge in the case of water is 1.89 for Zn^{2+} and 1.96 for Mg^{2+}, which indicates a significantly increased charge transfer with Zn^{2+}. For Me_2CO, the atomic charge on Zn^{2+} is 1.65, which indicates a much larger charge-transfer contribution. The predicted geometry for $Zn(Me_2CO)^{2+}$ (structure 5, Figure 4) is also different. The Zn−O−C angle is 134° and not 180°, as is the case for the complexes involving Mg^{2+} and Ca^{2+}. The ligand dipole is no longer aligned with the cation−oxygen bond, as was the case for $Mg(Me_2CO)^{2+}$, $Ca(Me_2CO)^{2+}$, and $Zn(H_2O)^{2+}$. The increased charge transfer and the change in geometry are related to a better alignment of the empty sdσ orbital on Zn^{2+} and the energetically more labile lone electron pair, located mainly on the in-plane p orbital of oxygen. The complete alignment with that pair would have led to a 90° angle. However, because of electrostatic repulsion between the Zn^{2+} and the partially positive hydrogens and C−O carbon, a compromise leads to the larger 134° angle. It is interesting that in protonated acetone, in which the electrostatic repulsion is less due to the smaller charge on the proton, the predicted angle is 113°,[21] which is much closer to the p orbital angle.

The linear $Zn(Me_2CO)^{2+}$ complex was also calculated and provides interesting comparisons. The linear complex, which is 6.5 kcal/mol less stable than the bent complex, has one imaginary frequency that corresponds to the movement of Zn away from the dipole axis. The Zn−O bond distance is 1.77 Å, and the atomic charge of Zn is 1.86 in the linear complex as compared to a bond distance of 1.87 and a cation charge of 1.65 in the bent complex (see Table 2). These results indicate that the overlap of the Zn with the energetically favorable

(19) Bauschlicher, C. W.; Sodupe, M.; Partridge, H. *J. Chem. Phys.* **1992**, *96*, 4453.

(20) Hartmann, M.; Clark, T.; van Eldik, R. *J. Am. Chem. Soc.* **1997**, *119*, 7843.

(21) Lee, E. P. F.; Dyke, J. M. *J. Chem. Soc., Faraday Trans.* **1992**, *88*, 2111.

orbitals on oxygen is smaller for the linear $Zn(Me_2CO)^{2+}$ complex than for the bent complex.

For $Zn(MAcA)^{2+}$, a combination of charge transfer and electrostatic binding similar to that in Me_2CO might be expected. Due to the electron shift from the nitrogen p orbital to the oxygen, a larger charge transfer component might seem reasonable, so that the essentially same amount of charge transfer for Me_2CO (1.65) and MAcA (1.69), predicted on the basis of the atomic charges for Zn^{2+} (see Table 2), is initially somewhat surprising. However, the electron shift, which is primarily responsible for the increased dipole of MAcA, involves orbitals that are orthogonal to the energetically labile oxygen p orbital in the plane and might not affect it energetically. So it is quite possible that the energy of the in-plane p orbital is very similar to that in Me_2CO and the charge transfer would then be expected to be similar. In addition, the dipole in MAcA is no longer along the C−O bond but, instead, is closer to the Zn−O bond, which increases the electrostatic aspects of the bonding interaction. Consequently, charge transfer becomes energetically more expensive, because each additional amount of charge transferred reduces the electrostatic contribution more significantly in MAcA than in Me_2CO. These observations, a similar energy gain from charge transfer in both Me_2CO and MAcA, and an increased cost of charge transfer due to the improved electrostatics in MAcA can then rationalize the predicted small decrease of charge transfer in MAcA (see Table 2) relative to Me_2CO, assuming that the NPA charges are reliable.

The rationale used to explain the convergence of the bond enthalpies between Ca and Mg complexes with increasing *n*, the difference in ligand−ligand repulsion, does not work in the case of Zn and Mg complexes due to the similar cation size. Point-charge calculations indicate that the ligand−ligand repulsion for $Zn(H_2O)_2^{2+}$ is less than 3 kcal/mol, which is similar to that in $Mg(H_2O)_2^{2+}$. The two effects, loss of ion core polarization and ligand−ligand repulsion, would therefore be expected to be similar for Mg and Zn water complexes. However, the bond enthalpy decrease from $Zn(H_2O)^{2+}$ to $Zn(H_2O)_2^{2+}$ is larger than that for the Mg analogue (15.1 kcal/mol vs 9.8 kcal/mol, see Table 1). NPA charges (see Table 2) indicate that Zn^{2+} does accept charge from the first and second water ligand. The ion-charge reduction with the addition of the second water ligand would result in a decreased electrostatic attraction, even at identical bond lengths. A model that includes ion−dipole and ion−induced-dipole interactions indicates that the energy loss due to the charge reduction, indicated by NPA charges, amounts to approximately 8 kcal/mol. In addition, indications are that the 4s orbital for Zn increases in energy, making subsequent charge transfers less energetically favorable. The combination of those two charge-transfer effects could account for the bond enthalpy drop. For the third addition of a water ligand, the bond enthalpy drop for Zn^{2+} is very large, 32.2 kcal/mol vs 15.4 kcal/mol for Mg (see Table 1). In addition to the increased ligand−ligand repulsion, as discussed for the Mg system, an equally important cause for the large drop is likely to be the same as for the Cu^+ system: the loss of the sdσ hybridization.[18] Also of note is the indication from the NPA charges that no additional charge transfer occurs for the third and fourth water ligand, which might help explain why the bond enthalpy for the third and fourth water ligand is lower for Zn than it is for Mg, despite the smaller Zn−O bond distance as compared to Mg−O (see Table 2 and Figure 4). The charge transfers which allow such strong binding of the first and second ligand, result in a reduced ion charge and subsequent weaker binding for additional ligands.

The addition of a second acetone to Zn^{2+} results in a very large enthalpy decrease of 48.6 kcal/mol. As discussed above for water as ligand, the sdσ hybridization of Zn^{2+} results in a ligand bond distance for two ligands that is closer than the ion−ligand distance for one ligand (see structures 5, 10, and Table 2). The bond distances for the Zn system are similar to those for the analogous Mg complex, so that loss of ion core polarization and ligand−ligand repulsion should be of similar magnitude. As was the case for the $Zn(H_2O)_2^{2+}$ case, the explanation is likely the result of charge transfers from Me_2CO to Zn^{2+}. But unlike the water system, in which the second ligand was also transferring charge to Zn, for Me_2CO, the NPA charges (see Table 2) indicate that the second Me_2CO does not transfer any additional charge. The orientation of the two acetone ligands has also changed slightly, compared to the mono-ligand case, and the Zn−O−C bond angle is 141.1° vs 133.8° (structures 5, 10). Such a structural reorientation increases the electrostatic contribution. The atomic charges (see Table 2) indicate that Zn^{2+} does not accept charge transfer beyond a certain limit (approximately 0.35 units of charge). It is possible that the resulting orbital energy increase from additional charge transfer becomes energetically unfavorable, particularly because it also lowers the electrostatic contributions to the bond enthalpy. The result is that for $Zn(Me_2CO)_2^{2+}$, the charge-transfer contribution from each ligand has been decreased by one-half as compared to the monoligand complex. Because charge transfer is such an important contribution to the bond enthalpy in $Zn(Me_2CO)^{2+}$, the loss of any additional contribution from the second ligand could explain such a large enthalpy decrease, despite the presence of sdσ hybridization. Similar to the enthalpy trend for water but more strongly, the presence of significant charge transfer increases the bond enthalpy for the first ligand (compared to Mg) but leads to much weaker binding already for the second ligand.

(b) Comparison of Experimental, Sequential Bond Energy Data $\Delta H^\circ_{n,n-1}$, $\Delta G^\circ_{n,n-1}$ and $\Delta S^\circ_{n,n-1}$ for M^{2+} (Mg, Ca, Zn, Sr, Ba) and Ligands L (H_2O, Acetone, *n*-Methylacetamide). The trend of bond enthalpy equalization, observed for $n = 1$ through $n = 4$ and discussed in the theoretical section, is fully realized for the experimentally observed bond enthalpies for $n = 5$ and $n = 6$ ligands. Figures 5 and 6 show experimental and theoretical bond enthalpies for $Mg(L)_n^{2+}$ and $Ca(L)_n^{2+}$, respectively, which illustrates the decrease of the bond enthalpies $\Delta H^\circ_{n,n-1}$ with *n* and their convergence at higher *n* for ligands L = Me_2CO, MAcA, and H_2O. Even reversals of the bond enthalpy trends that occur for complexes of lower *n* are observed at higher *n*. For example, for the (6,5) steps of acetone, a complete reversal of stability is observed (see Figures 2, 3, and Table 1), which is also reflected in the $\Delta G^\circ_{6,5}$ values at 298 K, which are Zn^{2+}, 9.0; Mg^{2+}, 11.9; and Ca^{2+}, 15.0 kcal/mol. For MAcA, $\Delta G^\circ_{6,5}$, Zn, 13.7; Mg, 13.5; and Ca, 14.5; there is also a reversal, however not a complete one, because Zn^{2+} provides a slightly stronger bond-free energy than Mg^{2+}. The (7,6) bond-free energies exhibit even more extreme reversals, particularly so for Me_2CO. Thus, Sr^{2+} and Ba^{2+}, which are very weakly bonding at low *n*, due to their large size,[1] lead to the strongest bonding: $\Delta G^\circ_{7,6}$, Ba, 9.1; Sr, 8.0; Ca, 6.3; Mg, 6.9; Zn, 7.0.

Clearly the reversals at high *n* must be connected with the inner-to-outer-shell transitions, which occur at higher *n* in an expected order: Zn, Mg, Ca, Sr, and Ba. Crowding of the inner shell and transitions to the outer shell occur earlier for the smaller ions and are responsible for these reversals. In the earlier work on the M^{2+} hydrates,[1,5] the theoretical results of Pavlov et al.[5] showed that for Zn^{2+}, the transition to an outer shell

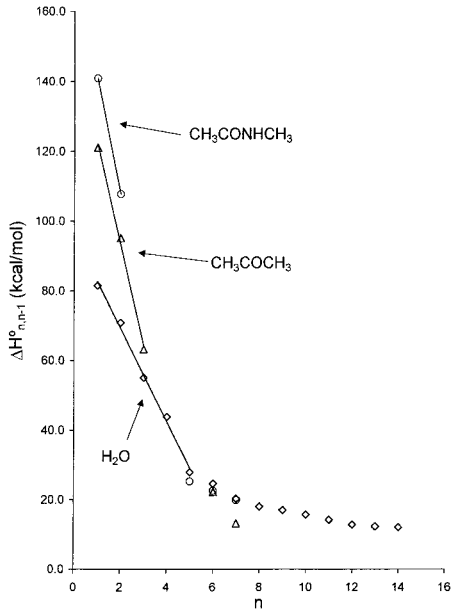

Figure 5. Bond enthalpies $\Delta H^\circ_{n,n-1}$ for $Mg(L)_n^{2+}$ complexes for which L = CH_3COCH_3 = Me_2CO (△), L = $CH_3CONHCH_3$ = MAcA (○), and L = H_2O (◇). Lines at low *n* are drawn as a guide to the eye. At low *n*, bond strength decreases in the order MAcA, Me_2CO, H_2O. More rapid decrease of bond energy with *n* occurs for the more strongly bonding MAcA and Me_2CO, such that an equalization of $\Delta H^\circ_{n,n-1}$ is observed for $n = 5, 6$. Transition to an outer shell at $n = 7$ is indicated by the $\Delta H^\circ_{n,n-1}$ and $\Delta S^\circ_{n,n-1}$ changes (see text). Inner-outer shell H-bonding, which occurs for H_2O and MAcA is indicated by a very gradual decrease of $\Delta H^\circ_{n,n-1}$ above $n = 6$. For Me_2CO, in which such a bonding is not present, a rapid fall-off is observed.

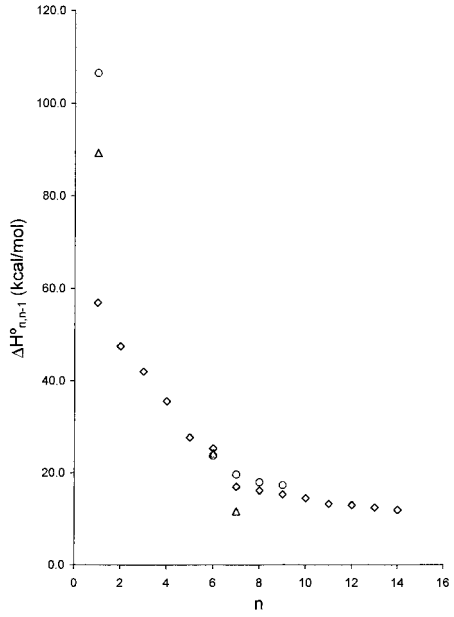

Figure 6. Bond enthalpies $\Delta H^\circ_{n,n-1}$ for $Ca(L)_n^{2+}$ complexes in which L = CH_3COCH_3 = Me_2CO (△), L = $CH_3CONHCH_3$ = MAcA (○), and L = H_2O (◇). At low *n*, bond order MAcA > Me_2CO > H_2O is the same as for Mg^{2+}; however, the bond energies for Ca^{2+} are lower than those for Mg^{2+}. More rapid fall-off of $\Delta H^\circ_{n,n-1}$ with *n* for MAcA and Me_2CO leads to an equalization at $n \approx 6$. Transition to an outer shell occurs at $n = 7$. Hydrogen bonding of outer-shell to inner-shell ligands leads to a very gradual fall-off of $\Delta H^\circ_{n,n-1}$ values for $n > 6$ for H_2O and MAcA, although a rapid fall-off is observed to Me_2CO, where such a bonding cannot occur.

occurred at the fifth water molecule. Thus, the energy for the structure $Zn(H_2O)_4(H_2O)^{2+}$ was shown to be lower than the directly bonded structure, $Zn(H_2O)_5^{2+}$. For Mg^{2+} and Ca^{2+}, the transition to an outer shell was shown to occur at the seventh molecule, that is, the energy of the structures $M(H_2O)_6(H_2O)^{2+}$ was shown to be lower than the directly bonded $M(H_2O)_7^{2+}$ structure.[5] However, for Mg with 6 water ligands, Pavlov et al,[5] as well as Rodriguez-Cruz et al.,[22] have shown that structures with 4 inner-shell waters and 2 outer-shell waters (4,2) and 5 inner-shell waters and 1 outer-shell waters (5,1) have only slightly higher energies than that for the 6,0 structure. Because the 4,2 and the 5,1 structures are entropically favored, Rodriguez-Cruz et al. have argued that their experiments indicate that at low temperatures, the 6,0 isomer dominates, but at higher temperatures, either the 4,2 or 5,1 isomer is prevalent.[22] The experimental measurements[1] which provided data for Mg, Ca, Sr, and Ba were in agreement with the theoretical predictions of the inner-outer-shell transitions for Mg and Ca and also demonstrated that for Sr, up to seven molecules could be fitted into the inner shell, although for Ba the number could be as high as 8 or 9.

Table 3. Selected Bond Enthalpies and Entropies from Table 1 to Illustrate the Transition to the Second Shell

Ca^{2+}	ΔH° kcal/mol	ΔS° cal/degree mol
$Ca(H_2O)_{6,5}$	25.3	31.1
$Ca(H_2O)_{7,6}$	16.9	20.2
$Ca(Me_2CO)_{6,5}$	24.5	30.9
$Ca(Me_2CO)_{7,6}$	11.6	17.8
$Ca(MAcA)_{6,5}$	23.7	30.9
$Ca(MAcA)_{7,6}$	19.6	27.7

Most of the present results for Me_2CO and MAcA can be explained if the shell occupation numbers for H_2O are assumed also to hold for these ligands. The transition from an inner to an outer shell does not depend only on the size of the metal ion and ligand but also on the type of non-covalent bonding between inner- and outer-shell ligand molecules. Due to the presence of two methyl groups in acetone, the outer-shell molecules in the acetone complexes cannot hydrogen bond to the inner-shell molecules. On the other hand, hydrogen bonding can occur for both H_2O and MAcA. Therefore, one can expect that bond energy decreases when a transition to the outer shell occurs will be most pronounced for Me_2CO. The available experimental data for acetone, Mg^{2+}, and Ca^{2+}, for which the transition to an outer shell occurs at the seventh molecule, fully support this expectation. The clearest results are obtained for Ca^{2+}. A very large drop is observed between $\Delta G^\circ_{6,5} = 15.0$ kcal/mol and $\Delta G^\circ_{7,6} = 6.3$ kcal/mol, for Ca-acetone. For Ca-MAcA, this drop is much smaller: $\Delta G^\circ_{6,5} = 14.5$ kcal/mol and $\Delta G^\circ_{7,6} = 11.3$ kcal/mol. The difference for these two ligands is most directly illustrated in Figure 3, which provides the van't Hoff plots. Due to the absence of hydrogen bonding for acetone, the gap between the two acetone van't Hoff plots for the 6,5 and 7,6 equilibria is very wide. On the other hand, for MAcA, due to hydrogen bonding, the (6,5), (7,6), (8,7), and (9,8) occur closely spaced and within the acetone (6,5)−(7,6) gap.

Special insights are provided by an examination of the specific ΔH° and ΔS° values in the region of the transition to the outer shell for Ca^{2+} and the three ligands, H_2O, Me_2CO, and MAcA. These results from Table 1 are detailed in Table 3. The much larger drop for the enthalpy change involving acetone is due, as already discussed, to the absence of H bonding of the outer-shell acetone to the inner-shell acetone ligands. The $\Delta H^\circ_{6,5}$ (MAcA) = 23.7 kcal/mol is smaller than that for H_2O, 25.3

(22) Rodriguez-Cruz, S. E.; Jockusch, R. A.; Williams, E. R. *J. Am. Chem. Soc.* **1999**, *121*, 8898.

kcal/mol, and this is probably due to the larger repulsion of the MAcA in the (crowded) six shell. On the other hand, $\Delta H^\circ_{7,6}$ (MAcA) = 19.6 kcal/mol is larger than that for H_2O, 16.9 kcal/mol. This difference shows that a stronger hydrogen bond is formed between the inner- and outer-shell MAcA molecules relative to the inner-outer-shell H_2O molecules. Stronger H bonding for MAcA is expected because it involves a carbonyl oxygen of the outer MAcA molecule, which is a better H acceptor than the oxygen of the water molecule. The N−H hydrogen of the inner MAcA involved in the hydrogen bond also may be more acidic than the hydrogen of a water molecule, thus further strengthening the H bond for the MAcA system relative to that for H_2O. However, a greater acidity of the inner-shell MAcA molecules relative to H_2O molecules may not be present. While the NH hydrogen will be more acidic than the O−H hydrogen in the isolated molecules, the presence of Ca^{2+} promotes additional protic character of the ligands' hydrogens, and that effect may be stronger on the small H_2O molecules.

The entropy changes for the Ca^{2+} (6,5) and (7,6) transitions for H_2O as ligand were examined in the earlier study.[1] The very low $\Delta S^\circ_{7,6}$ = 20.2 cal/mol·K indicates that the outer-shell water molecule is much more free. This freedom was rationalized[1] by the following considerations.

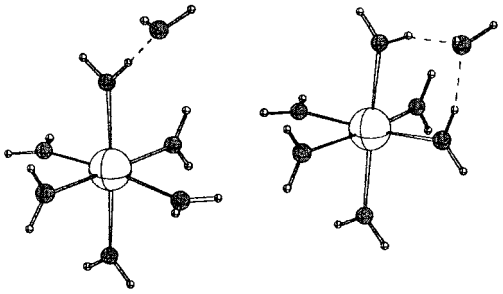

11 12

Two structures of close to equal free energy, 11 and 12, are predicted by the theoretical calculations[5] for $Ca(H_2O)_6(H_2O)^{2+}$. It was argued[1] that the transition state between these two structures is also of similar free energy and, therefore, the transition between 11 and 12 can be very facile. Such transitions lead to a high mobility of the outer molecule, resulting in a quasi translation over the "surface" of the inner shell. Such a free motion leads to a low $\Delta S^\circ_{n,n-1}$. The very low $\Delta S^\circ_{7,6}$ = 17.8 cal/mol·K for Ca and Me_2CO can also be rationalized on the basis of a very free quasi-translation of the outer-shell acetone molecule over the "surface" provided by the inner-shell Ca $(Me_2CO)_6^{2+}$ complex. Due to the absence of hydrogen bonding, the outer acetone molecule is very weakly bonded, and such a quasi-free translation can be expected. For MAcA, a rather high $\Delta S^\circ_{7,6}$ = 27.7 cal/mol·K is observed. Strong hydrogen bonding is indicated by the corresponding enthalpy change. The structure 13 of $Ca(MAcA)_6^{2+}$, when compared to the hydrate structures 11 and 12, provides good grounds for an argument that a quasi-translation is not possible for MAcA.

There are only half as many protic hydrogens in $Ca(MAcA)_6^{2+}$ than is the case for $Ca(H_2O)_6^{2+}$. Furthermore, the free rotation of an inner-shell water molecule which is required for the transition between the water structures 11 and 12 would be replaced by a hindered rotation in the MAcA structure 13. These two factors could be expected to make the transfer of the outer MAcA molecule from one H bond site to the other considerably more difficult. Therefore, a quasi-translation cannot

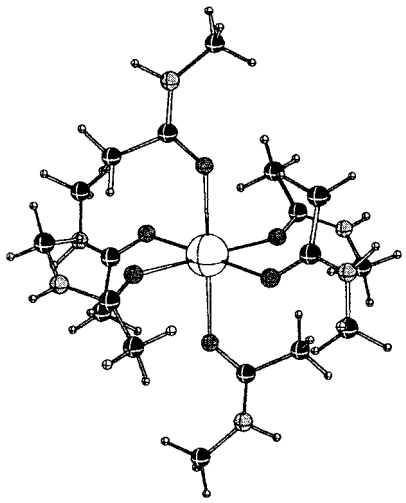

13 $Ca(MAcA)_6^{2+}$ (B3LYP/LANL2DZ).

be expected for the MAcA complex. This is in line with the observed rather large $\Delta S^\circ_{7,6}$ = 27.7 cal/mol·K. A double hydrogen bond structure analogous to structure 12 for water would make the outer molecule even less free. However, such a structure is compatible with an entropy change that is higher[1] than the observed $\Delta S^\circ_{7,6}$ = 27.7 cal/mol·K; moreover, suitable protic hydrogens (H−N) for such a complex are likely to be too far apart to allow two hydrogen bonds to a single C=O oxygen. Therefore, the single hydrogen bonded structure analogous to structure 11 is indicated to be the dominant structure for $Ca(MAcA)_6(MAcA)^{2+}$.

The changes between $\Delta H^\circ_{6,5}$ = 23.3 kcal/mol, $\Delta H^\circ_{7,6}$ = 13.6 kcal/mol and $\Delta S^\circ_{6,5}$ = 34.8 cal/mol·K, $\Delta S^\circ_{7,6}$ = 22.4 cal/mol·K (Table 1) for Mg^{2+} and acetone are similar to those for Ca^{2+} and acetone, although somewhat less pronounced. This indicates that the transition to an outer shell where the outer molecule is quite free occurs not only for Ca^{2+} and acetone but also for Mg^{2+} and acetone. Comparison of the (6,5) and (7,6) values of Mg^{2+} and MAcA with those for Ca^{2+} and MAcA shows that these are also similar. However, hydrogen bonding and reduced ligand−ligand repulsion in 4,2 and 5,1 complexes, as compared to the 6,0 structure, could offset the loss of the attractive electrostatic interaction. Therefore, it is possible that for the Mg-MAcA system the transition to a second shell occurs earlier. For the analogous Mg-H_2O system, discussed earlier, indications are that the transition is temperature-dependent. Because MAcA is more bulky than H_2O and is capable of stronger hydrogen bonding, the transition to an outer shell may be energetically favorable even at 0 K. Our experimental results cannot give a definite answer, but an inner shell with six MAcA could be expected to be more crowded than a corresponding shell with six Me_2CO, which should lead to a larger $\Delta S^\circ_{6,5}$ for MAcA. The lower $\Delta S^\circ_{6,5}$ for $Mg(MAcA)_6^{2+}$ (30.8 cal/mol·K), as compared to $Mg(Me_2CO)_6^{2+}$ (34.8 cal/mol·K), could indicate that 5,1 or 4,2 structures are at least competitive with if not dominant to the 6,0 structure.

There are also similarities between the (6,5) and (7,6) values for acetone between Zn^{2+} and Mg^{2+}, but they are less consistent. Thus, $\Delta H^\circ_{6,5}$ = 17.4 kcal/mol (Zn^{2+}) is considerably smaller than $\Delta H^\circ_{6,5}$ = 22.3 kcal/mol for Mg^{2+}, although the $\Delta H^\circ_{7,6}$ = 14.4 kcal/mol (Zn^{2+}) is higher than $\Delta H_{7,6}$ = 13.6 kcal/mol (Mg). Also, the entropy changes for Zn^{2+}, $\Delta S^\circ_{6,5}$ = 28.5 cal/mol·K and $\Delta S^\circ_{7,6}$ = 24.6 cal/mol·K, are far less indicative of a transition to an outer shell where there is much greater freedom than was the case for Mg^{2+} and particularly Ca^{2+}. Therefore,

the transition to an outer shell for Zn^{2+} with acetone or MAcA probably occurs earlier, for example, with the fifth molecule. Unfortunately, data for the (4,3) changes are not available to provide more solid confirmation.

(c) Applications to Biochemistry. Mg^{2+} and particularly Ca^{2+} play a most important role in biological processes.[23,24] Of special interest is the participation of Ca^{2+} and Mg^{2+} in muscle relaxation and contraction, in which Ca^{2+}-binding proteins, such as muscle-calcium-binding parvalbumin (MCBP) are involved. This group of proteins has a common Ca^{2+}-binding motif of two helices that flank a loop of 12 contiguous residues. The 12 residues provide the six oxygen ligands that bind to Ca^{2+}. Backbone carbonyl oxygens from these residues do participate in the Ca^{2+} bonding; however, most often, only one of the oxygens[24] comes from that source, although there are cases where two or three carbonyl oxygens participate. The carboxy group of acidic residues such as aspartic acid (Asp) and glutamic acid (Glu) is also involved as a ligand and in some proteins, such as MCBP, provides as much as four of the total six ligands, a minimum of one carboxylic group being always present. Hydroxy ligands such as serine and threonine, as well as water molecules, provide the rest of the ligands (see Table 2 in Kretsinger[24]).

In a previous study involving Zn metalloenzymes and particularly carbonic anhydrase,[9a] we inquired about the relationship between the bond strength and the function of the Zn-bonding ligands. On the basis of theoretically and experimentally determined bond energies for the three directly bonding histidine (His) ligands and the fourth H_2O ligand, we were able to show that the three very strongly bonding His ligands provide a high Zn affinity which prevents the escape of Zn^{2+} into the surrounding aqueous medium. A second and also vital function of these ligands is to reduce the bonding of the fourth, H_2O, ligand to a given low bond energy value which is exactly suited to the participation of this ligand in the catalyzed conversion of H_2O and CO_2 into H_2CO_3.

The establishment of a relationship between ligand bond energies and function would be also most desirable for the Ca^{2+} and Mg^{2+} host proteins discussed above. Unfortunately, the situation is much more complicated for these systems due to two essential differences: (a) Only one ligand type (His) is involved as a directly bonding nonreactive ligand in carbonic anhydrase, while for Ca^{2+} and Mg^{2+}, a large variety and a greater number of ligands are present. The binding energies for the specific complement of ligands, thus, need to be known. (b) The position of the metal Zn ligand complex in carbonic anhydrase was in the center of the globular protein, and this made for relatively easy inclusion of the effect of the protein and aqueous environment on the bond energies. For Ca^{2+}, Mg^{2+}, and the above proteins, the position of the metalloligand complex is not in the middle of a globular protein but is much more irregular, such that the complex may be accessible to direct strong solvation effects by the aqueous environment. Under these conditions the inclusion of the total effect of the environment on the bond energies becomes much more difficult.

To address problem a, we have been successful in preparing by electrospray Ca^{2+} and Mg^{2+} ion ligand complexes in the gas phase that contain mixed ligands. These complexes did include one or more carboxylic acid groups. Thus, using acetic acid as a model of the aspartic or glutamic acid residue, complexes containing one or more acetic acids as well as MAcA or acetone and water molecules could be prepared, and some of the binding energies could be determined by ion equilibria. The acidic groups when single corresponded to the deprotonated acid, that is, the acetate, but when multiple, included only one deprotonated species such that the charge of the complex has $z = +1$. Ligand bond enthalpies and free energies obtained from ion−ligand equilibria of such Ca^{2+} and Mg^{2+} complexes as well as some limited theoretical results will be presented in a future publication.

Considering the extraordinary complexity of muscle Ca^{2+} and Mg^{2+} proteins and their function,[23,24] the present results are as yet probably insufficient to provide new insights for Ca^{2+} binding proteins such as MCBP.

The observed strong hydrogen bonding between inner- and outer-shell complexes, $M(MAcA)_6(MAcA)^{2+}$, for which bond enthalpies as high as 20 kcal/mol were observed for Mg^{2+} and Ca^{2+}, could be of biochemical significance, because it indicates the presence of extra strong hydrogen bonding between N−H···O═C peptide groups near the doubly charged ion. We have not been able to establish whether such effects are present in native Ca- and Mg-binding proteins.

IV. Conclusion

The experimental bond enthalpies and entropies confirm the preference of Ca for a six-ligand inner shell. For Mg, they are in agreement with observations that indicate 4-, 5-, and 6-ligand inner shells are competitive with respect to free energy. For Zn, the bond enthalpies and entropies of the Me_2CO and MAcA systems are consistent with a preference for a 4-ligand inner shell.

The bond enthalpy equalization trend between the predominantly electrostatic Ca- and Mg-ligand systems, discussed in the present paper, illustrate that ligand−ligand repulsion is the primary cause for the subsequent weaker ligand binding. The particular characteristics of the ligand, dipole, and polarizability are responsible for the strength of the electrostatic attraction but also for the strength of repulsion of subsequent ligands, so that the two opposite forces allow an equalization of bond enthalpies with increasing *n* between otherwise disparate ligands and ion centers. Zn allows, in addition to the electrostatics, significant charge transfer from some of the ligands. The charge transfer increases the attractive forces but also reduces the electrostatic attraction for subsequent ligands due to the diminished ion charge, so that again the two opposite forces allow an equalization with increasing *n* even with systems that exhibit only electrostatic binding, such as the present Ca and Mg systems.

These observations illustrate that bound ligands and their particular binding modes influence the binding strength and mode of subsequent ligands. This behavior is an important consideration for understanding the metal sites in biological systems. Because the present Ca and Mg systems contain only a single type of ligand, i.e., MAcA, which models the carboxylic backbone interaction, comparisons to biological systems in which the metal cation site generally contains mixed ligands with only one to three carboxylic backbone interactions are only very qualitative. Work is currently underway to obtain bond energies of mixed ligand systems that include a model ligand for carboxylic acid residues, which will allow more meaningful comparisons to the analogous biological systems.

JA002021Z

(23) Strynadka, N. C. J.; James, N. G. *Annu. Rev. Biochem.* **1989**, *58*, 951.

(24) Kretsinger, R. H. *Annu. Rev. Biochem.* **1976**, *916*, 239.